Solid Earth

Open Access

Supplement of

Velocity structure and the role of fluids in the West Bohemia Seismic Zone

C. Alexandrakis et al.

Correspondence to:

1   **Supplementary Figures**

2

3   **Velocity structure and the role of fluids in the West Bohemia Seismic**

4   **Zone**

5

6   **C. Alexandrakis[1], M. Calò[2], F. Bouchaala[3], and V. Vavryčuk[4]**

7   [1]{Institute of Geophysics and Geoinformatics, TU Bergakademie Freiberg, Freiberg, Germany}

8   [2]{Berkeley Seismological Laboratory, Berkeley, United States of America}

9   [3]{The Petroleum Institute, Abu Dhabi, United Arab Emirates}

10   [4]{Institute of Geophysics, Czech Academy of Science, Prague, Czech Republic}

11   Correspondence to: C. Alexandrakis (catherine.alexandrakis@geophysik.tu-freiberg.de)
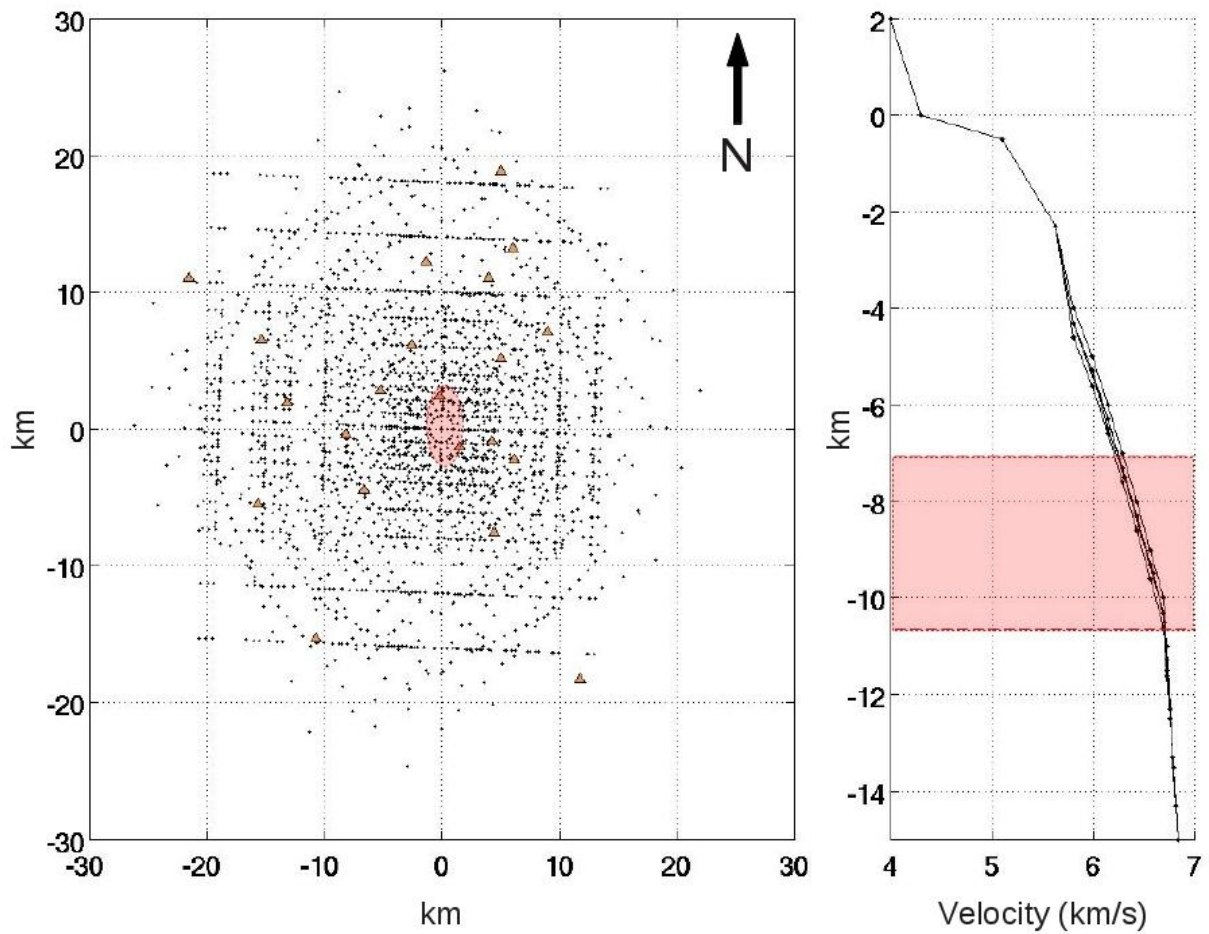
12

2
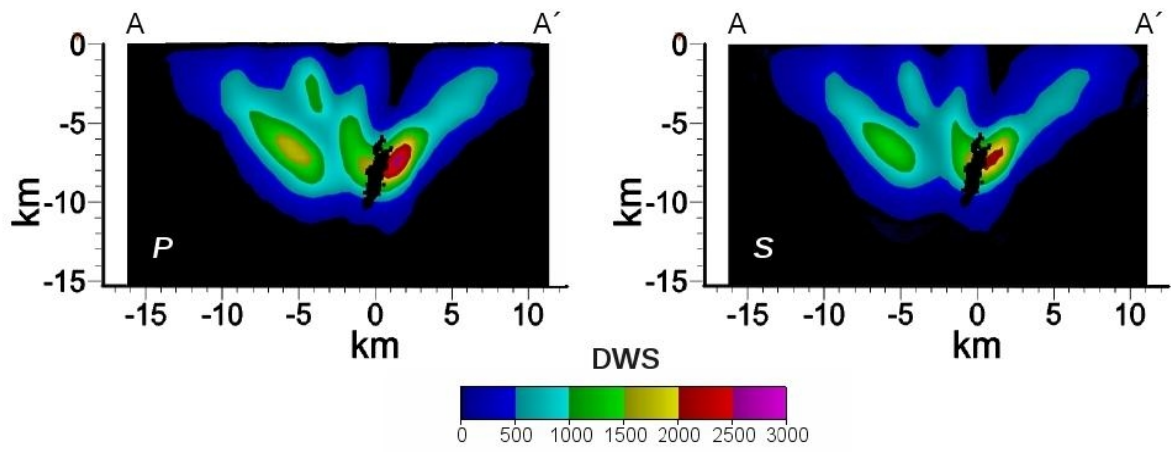
3   Supplementary Figure 1. Derivative Weight Sum (weighted hit count; Toomey and Foulger 1989)

4   for the *P* and *S* traveltime datasets for profile A-A´. Maximum DWS for P and S are 12605 and

5   10803, respectively.

2

3   Supplementary Figure 2. Summary of all (a) lateral nodes and (b) depth nodes and *P*-wave velocity

4   models used in the Weighted Average Model (WAM) calculation. Location of the 2008 earthquake

5   swarm is noted by the oval in (a) and shading in (b). Inversion nodes and stations are marked by

6   small crosses and triangles, respectively.

2
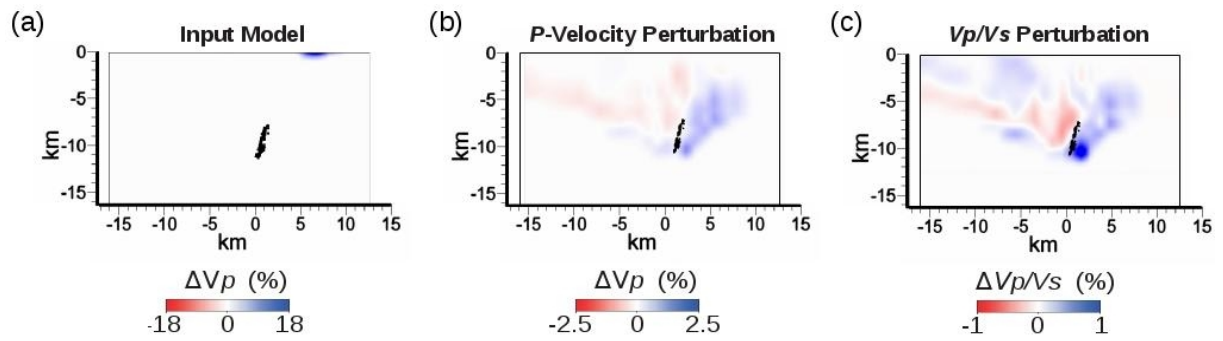
3　Supplementary Figure 3. Synthetic test illustrating the insignificant effects of near-surface velocity

4　heterogeneitites. In the input model (a), the velocity at 0.5 km depth is extended up to the surface (z

5　= 0 km), mimicking an outcrop of bedrock. All velocities and ratios outside of the perturbed area

6　correspond to the regional model of Málek et al. (2001). This results in a local *P*-velocity increase

7　of 18%. The recovered *P*-velocity (b) and *Vp/Vs* models (c) show minor perturbations (less than

8　2.5% and 1%, respectively).

2
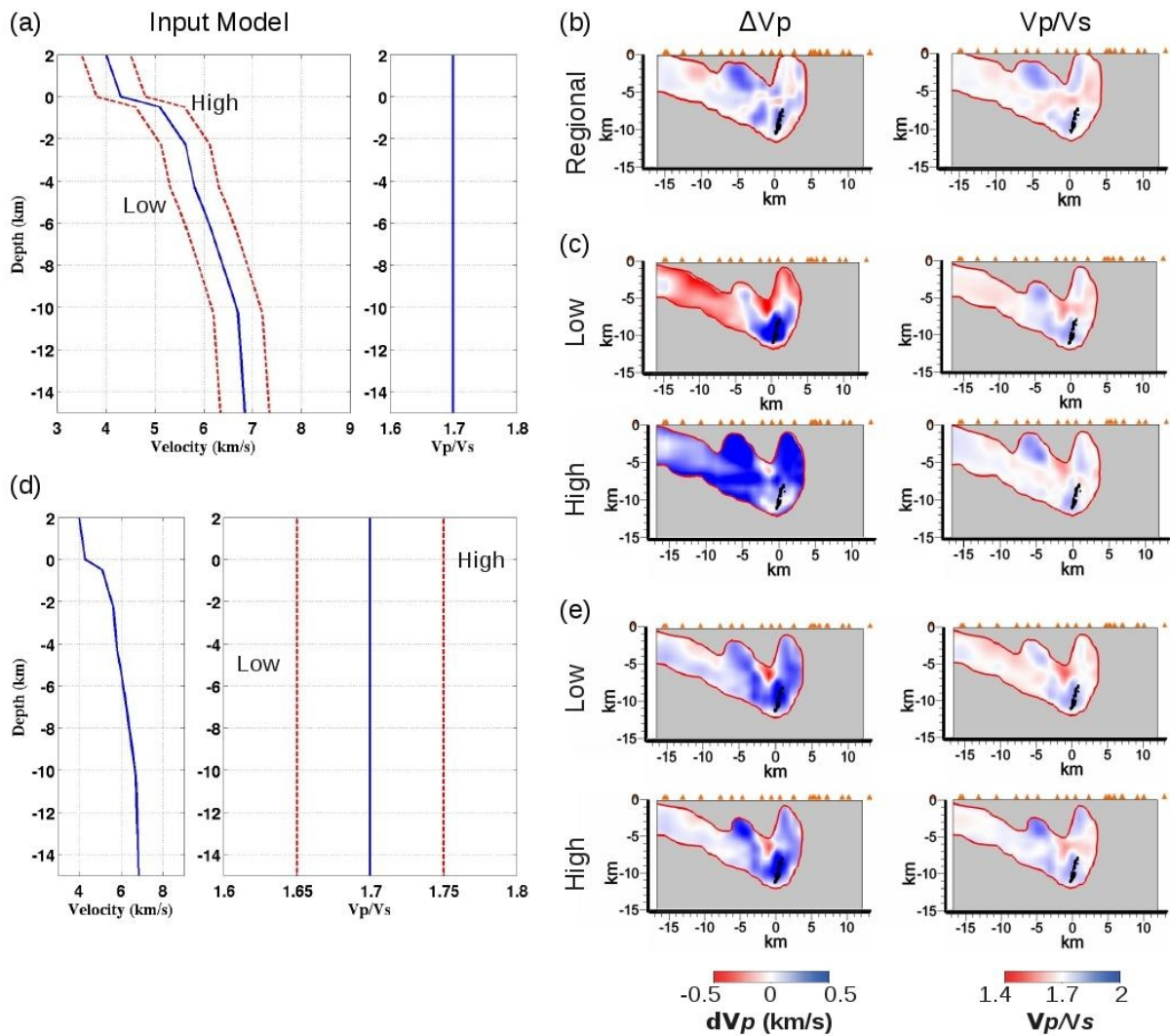
Supplementary Figure 4. Test on input model dependence. First the regional model of Málek et al. (2001) (blue lines in a and d) is used as the tomography starting model (b). When the input model's *P*-velocity is perturbed (red lines in a), the calculated *P*-wave velocity models (c) show a strong dependence. However, the calculated *Vp/Vs* ratio models show minor dependence below 5 km. When the regional *P*-wave velocity model is used, but the input *Vp/Vs* ratio is perturbed (d), the calculated models (e) show less dependence. Profile A-A' is shown. Only areas constrained by the data are shown. *P*-wave velocity tomography plots are shown with respect to the regional model.

2
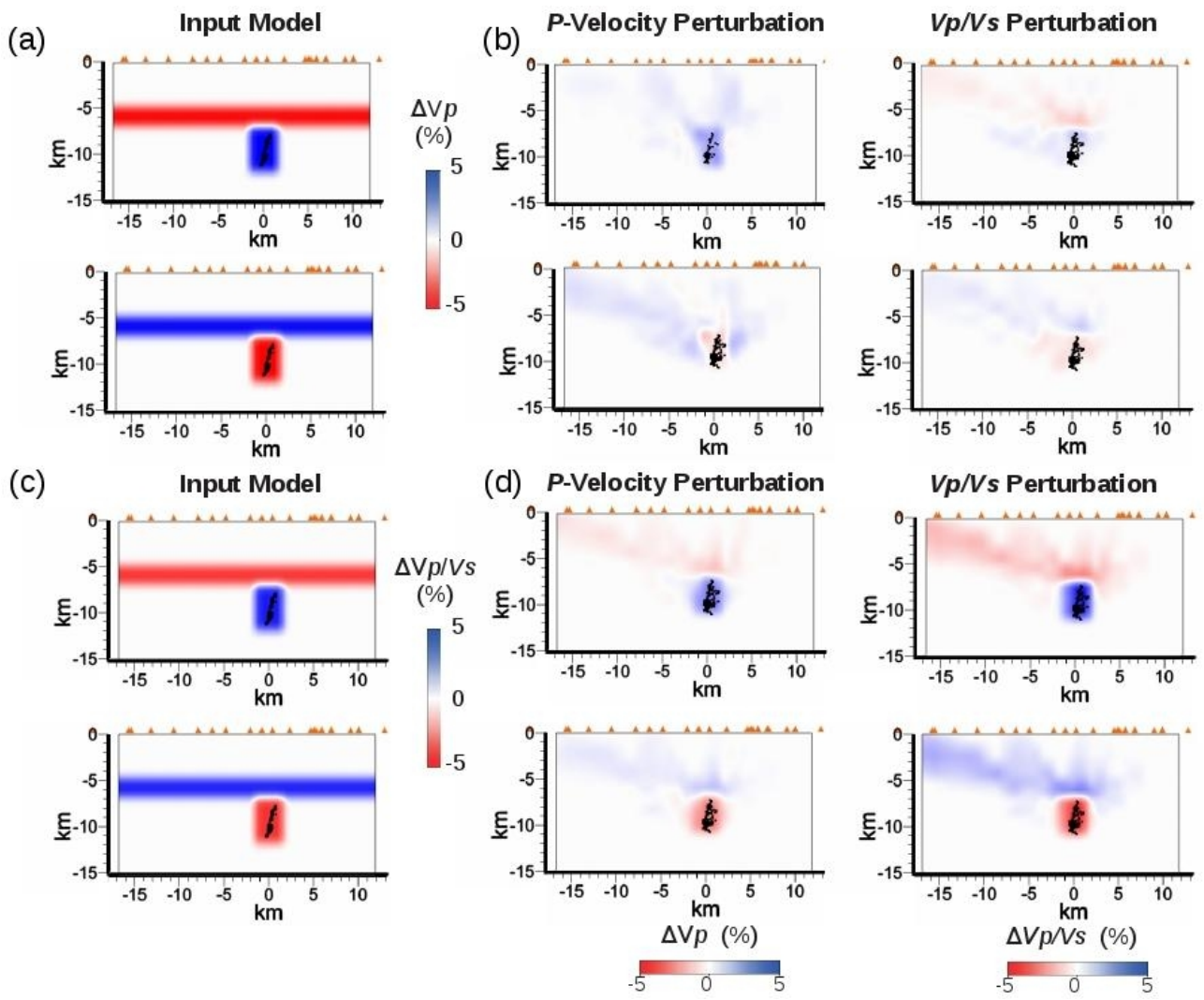
3   Supplementary Figure 5. Anomaly restoration synthetic test. Same models as for Fig. 4 with a 2 km-

4   thick, contrasting layer inserted over the anomaly (a and c). As with the previous tests, the

5   calculated *Vp/Vs* models show better anomaly recovery than the calculated *P*-wave velocity models.

(a) P-Wave WAM Model

(b) S-Wave WAM Model

2
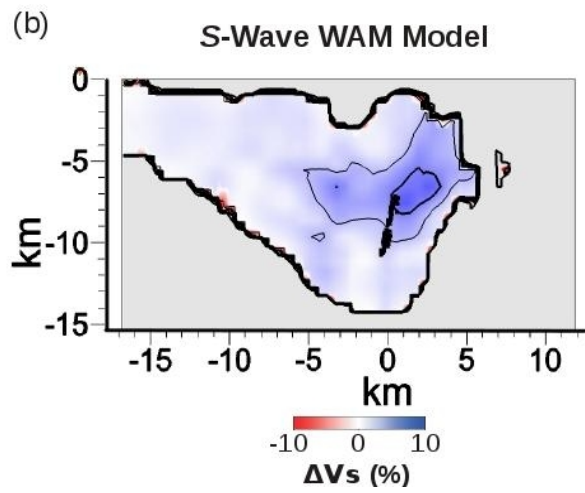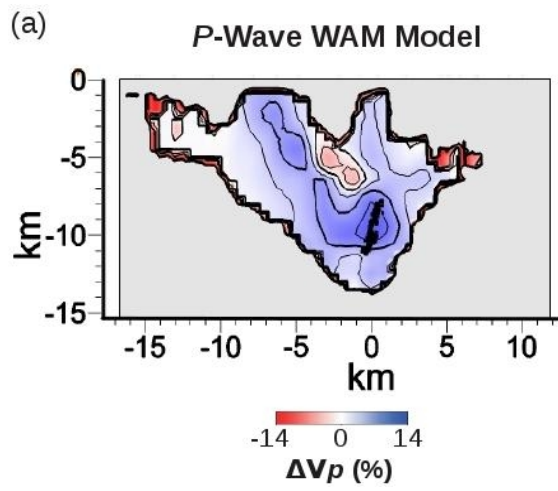
Supplementary Figure 6. Across-strike profile (A – A') for the calculated *P*-wave (a) and *S*-wave (b)

velocity Weighted Average Models. Only areas constrained by the data are shown. Earthquake

hypocenters are projected onto the profiles.